FINAL PUBLISHABLE REPORT

Grant Agreement number	17FUN10
Project short name	ParaWave
Project full title	Josephson travelling wave parametric amplifier and its application for metrology

Project start date and duration:		01 July 2018, 42 months
Coordinator: Ralf Dolata, PTB Tel: + 49 531 592 2247 E-mail: ralf.dolata@ptb.de Project website address: https://sites.google.com/inrim.it/parawave		
Internal Funded Partners: 1. PTB, Germany 2. INRIM, Italy 3. NPL, United Kingdom	External Funded Partners: 4. LanU, United Kingdom 5. RHUL, United Kingdom	Unfunded Partners:
RMG1: INRIM, Italy (Employing organisation); NPL, United Kingdom (Guestworking organisation)		

TABLE OF CONTENTS

1 Overview

The emerging field of microwave quantum optics has gathered significant interest for the launch of technologies taking advantage of quantum mechanical phenomena, but its progress critically depends on the availability of cryogenic low noise amplifiers. This project has developed a favourable type of the Josephson Travelling Wave Parametric Amplifier (JTWPA) based on the three-wave mixing principle, offering high gain, large bandwidth and potentially quantum limited noise performance. The associated quantum amplifier metrology for the characterisation of JTWPAs was established and applications of the JTWPA to enhance the sensitivity of quantum sensors and as a source for quantum illumination were explored.

2 Need

Quantum technologies offer a step change in sensitivity or accuracy not attainable with classical devices. They promote transformative advances to science and society and have the capacity to improve the competitiveness of European industry and SMEs by creating new commercial opportunities in many of the world's biggest markets. Areas that will benefit the most include quantum computing, quantum communication and "quantum non-demolition" measurements. In addition, recent developments in quantum sensing, quantum information circuits, astronomical detection and modern communications rely on the precision detection of microwave photons. Furthermore, the emerging field of microwave quantum optics could be used to provide ultra-precise and metrological measurement. This is needed for the precise determination of single photon properties including timing and phase, and quantum properties such as squeezing and entanglement.

However, all these developments critically depend on the availability of cryogenic amplifiers with sufficient gain and bandwidth as well as added noise no larger than that determined by quantum-mechanical principles. Current state-of-the-art cryogenic semiconductor amplifiers have (at GHz frequencies) an electrical noise that is at least a factor of ten too high for quantum sensitive applications. Current superconducting quantum-limited microwave amplifiers available both commercially and in research laboratories all suffer from compromises in specification and hence a broadband quantum-limited microwave amplifier is urgently needed.

The Josephson Travelling Wave Parametric Amplifier based on the three-wave mixing, whose fundamentals were developed within this project, will achieve significant advances in the state-of-the-art gain, in bandwidth and simplicity of construction. Additionally, there is a need for a reliable metrological characterisation of JTWPA and similar devices, what will be established within this project. Investigating the capabilities of the JTWPA is a first step towards the advancement of microwave quantum optics, which could impact many fields of science and technology, such as artificial intelligence, cryptography, and brain scans.

3 Objectives

The overall goal of this project was to develop a novel and practical broadband microwave amplifier capable of operation at and beyond the fundamental, or standard quantum limit, of sensitivity.

The specific objectives of this project were:

1. **To develop a broadband JTWPA** utilising three-wave mixing, with a power gain of 20 dB and flatness of ±3 dB in a one octave range centred on 5 GHz to 6 GHz. The amplifier development will include optimisation of circuit design parameters and physical layout, the preparation of functional samples and optimisation of the fabrication technology. JTWPA circuits will be developed in Nb, Al and Nb-Al hybrid technology according to the intended application.
2. **To analyse the amplifier noise and demonstrate thermal noise-squeezing (up to 5 dB) and quantum-limited performance** (noise temperature better than, at least $hf/k_B \sim 0.3$ K), and to clarify the role of device parameters (nonlinearity and dispersion, signal gain, bandwidth and dynamic range) to optimise the amplifier operation.
3. **To develop reliable and validated quantum amplifier metrology** (components and processes) for the characterisation of the JTWPA device and other cryogenic amplifiers. The envisaged metrology platform will allow the characterisation of devices in terms of their gain, bandwidth and harmonic generation. Standard room temperature microwave sources and thermal noise sources will be used for metrological characterisation.

4. To improve the sensitivity of the JTWPA device to quantum levels with minimum backaction, through **integration with quantum sensors and macroscopic quantum systems**. In particular, to combine the JTWPA-based preamplifier with nanoSQUID sensors operating in a dispersive mode and rf-single-electron-transistor (rf-SET) charge detectors optimised for error counting in single electron pumps. Both, the SQUID and the superconducting SET (i.e., Cooper-pair transistor) are examples of macroscopic quantum sensors/systems since their behaviour involves a macroscopically large number of Cooper pairs. Further, to demonstrate frequency multiplexing in these circuits, and flux and charge sensitivities approaching the standard quantum limit.
5. **To facilitate the take-up of the technology and measurement infrastructure developed in the project** by the measurement supply chain (quantum technology professionals) and end users (electronics, healthcare, information and communications industries) including demonstration of the application of the JTWPA device in at least two quantum measurement case studies.

4 Results

4.1 Development of a broadband Josephson travelling wave parametric amplifier (JTWPA)

4.1.1 Design of JTWPA circuits

The design of JTWPA chips followed the basic concept of the publication "Josephson Traveling-Wave Parametric Amplifier with Three-Wave Mixing" [1], authored by PTB. Additional information about the general design of JTWPAs has been published in "Flux-driven Josephson traveling-wave parametric amplifier" [2]. Fig. 1 shows the basic design, a series array of rf-SQUIDs (radio frequency Superconducting Quantum Interference Devices) with ground capacitors C_0 forms a nonlinear high frequency transmission line. The use of rf-SQUIDs instead of single Josephson junctions or dc-SQUIDs allows for the tuning of the nonlinearity parameters by an external magnetic field and enables the advantageous three-wave-mixing in the JTWPA device. It is desirable to choose L_g and C_0 to get an impedance of 50 Ω. The SQUID screening parameter β_L of the rf-SQUIDs must be below 1, a good value might be about $\beta_L \approx 0.5$. The critical current of the Josephson-junctions should be in the range 1 µA < Ic < 5 µA to obtain convenient values for the inductors L_g. The SQUIDs and the ground capacitors C_0 are usually embedded in a coplanar waveguide (CPW) to provide easy connections with 50 Ω impedance. The number of SQUIDs N_s required to achieve the desired gain of 20 dB is on the order of 500 to 1500, depending on the chosen circuit parameters.

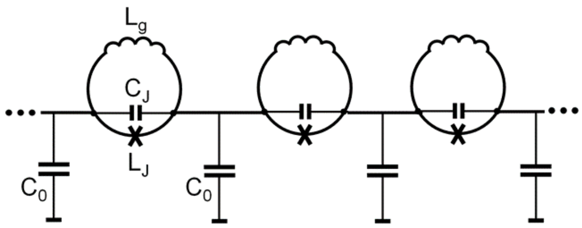

Geometrical inductor:	L_g	$Z_0 = (L_g/C_0)^{0,5} = 50\ \Omega$
Capacitor to ground:	C_0	
Critical current of JJs:	I_c	$\beta_L = 2\pi I_c L_g/\Phi_0 < 1$

Fig. 1: *Schematic electric circuit of the basic JTWPA design and fundamental design relations.*

The achievable gain of this basic circuit design is limited to a few dB. Because of small dispersion and high bandwidth of the transmission line the pump energy is preferably converted to the second and higher harmonics and other higher order mixing products, but only to a small extent into signal amplification. These effects were confirmed experimentally, and by circuit simulations using WRspice and a theoretical model [3]. Additional simulations have shown the effects of parameter variations and defects in JTWPA circuits [4].
To impede the amplification of signals with frequencies above the pump frequency a significant phase mismatch between the pump signal and the higher frequency signals, preventing their amplification, should be established. The project determined that this can be realised by an appropriate adjustment of the JTWPA circuit parameters to achieve a lower cut-off frequency and a smaller plasma frequency of the SQUIDs. In

particular C_j can be increased to create larger dispersion for the higher frequency components. Unfortunately, such circuit parameters also cause a small phase mismatch between the pump signal and the low frequency signals to be amplified, limiting the achievable gain. To avoid this undesired phase difference, the project worked out several alternative strategies:

(A) Resonant-Phase Matching

The unwanted phase difference between the pump and the signal to be amplified can be compensated for by using Resonant-Phase-Matching: i.e., the periodic inclusion of resonators with resonance frequency slightly below the pump frequency into the serial array of SQUIDs [5]. This concept modifies the phase velocity in the vicinity of the resonance frequency of the resonators and removes the destructive phase difference for a fixed pump frequency. The project verified this approach by circuit simulations and optimised the circuit parameters for achieving a high gain in a wide bandwidth. In the simulation the results looked very promising and a JTWPA power gain of more than 20 dB and flatness of ±3 dB in a 6 GHz bandwidth has been attained. Fig. 2 shows the revised circuit design and a selected set of parameters (not fully optimized yet), Fig. 3 the results of the WRspice simulation. In real circuits the gain is expected to be somewhat lower because of losses and deviations from the optimum circuit parameters.

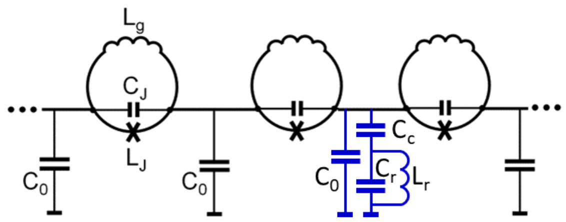

Geometrical inductor:	L_g = 100 pH	cut-off frequency:	f_0 = 50 GHz
Capacitor to ground:	C_0 = 100 fF	SQUID plasma frequ.:	f_j = 36 GHz
Impedance:	Z_0 = 32 Ω	No. of SQUIDs:	N_s = 500
(in optimum bias point Z ≈ 50 Ω)			
Critical current of JJs:	I_c = 2.5 µA	JJ capacitance:	C_j = 200 fF
Resonator capacitor:	C_r = 1 pF	Resonator inductor:	L_r = 172.5 pH
Coupling capacitor:	C_c = 40 fF	SQUIDs per resonator:	N_r = 4

Fig. 2: *Modified schematic of the JTWPA and a set of circuit parameters.*

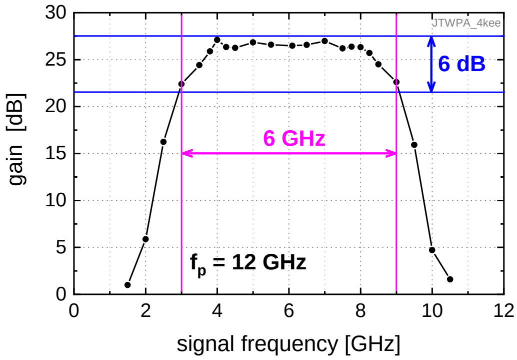

Fig. 3: *Simulated dependence of signal gain versus frequency for the parameter set of Fig. 2.*

A circuit design and layout, based on the Resonant-Phase-Matching concept and using lumped element LC resonators, has been developed for the fabrication in Nb-technology. Unfortunately, the fabricated samples were not functional due to shorts in the large area capacitors of the resonators and too high spread of circuit parameters. The production of many LC resonators with lumped elements is in principle feasible but represents a great challenge for the available fabrication technology. For this reason, the project is considering developing

another Resonant-Phase-Matching design, using quarter-wavelength CPW based resonators, promising higher yield and easier fabrication, since the need for a large number of big capacitors is avoided [6].
To investigate the effects of losses in circuit elements and the unavoidable spread of circuit parameters in the real fabrication process, thorough simulations have been performed on the Resonant-Phase-Matching concept by PTB, also considering the available dynamic range of the JTWPA. The results clearly demonstrate that it should be possible to create a high performance three-wave-mixing JTWPA based on the available state of the art fabrication technology and achieving the targeted high gain in a wide bandwidth. Detailed results of these simulations have been published in [7].

(B) Gap-Engineering (periodic loading)

The concept of Gap-Engineering was examined theoretically and by circuit simulations at PTB. By a periodic variation of circuit parameters, a gap in the rf-transmission of the JTWPA is created. Similar to the Resonant-Phase-Matching, this approach modifies the phase velocity in the vicinity of the frequency gap and compensates the phase difference between the pump and the signal to be amplified [8]. Fig. 4 shows the concept with a periodic modulation of the ground capacitors.

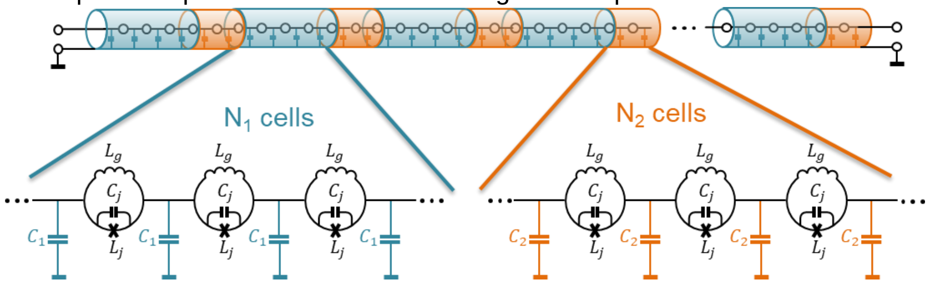

Fig. 4: *Schematic electric circuit of the JTWPA design including a periodic variation of the ground capacitors.*

A distinct advantage of the Gap-Engineering technique is that no additional circuit elements are needed, just the values of already present components must be periodically altered. Therefore, JTWPAs including the Gap-Engineering are relatively easy to fabricate. It was found that for obtaining a smooth dependence of the gain versus frequency in a wide band it might be favourable to create a second gap in the rf-transmission of the JTWPA to supress propagation of the second harmonic of the pump frequency. Using WRspice simulations, a power gain of more than 20 dB and flatness of ±3 dB is achieved in a bandwidth of about 7 GHz, clearly surpassing the original goal of a 4 GHz bandwidth. Another advantage of the Gap-Engineering technique in comparison with the Resonant-Phase-Matching is a significant larger margin for the pump frequency, what is believed to be very useful in practical applications. PTB investigated this approach extensively for the Three-Wave Mixing JTWPA and the results have been presented in a publication [9].

(C) Quasi-Phase-Matching

Another alternative approach has been invented by PTB [10]. It is based on the Quasi-Phase-Matching concept originally exploited in optical devices and has the advantage that no additional circuitry is required. Circuit fabrication should be relatively easy because only the spatial orientation of the basic rf-SQUID elements will be changed periodically. Fig. 5 explains the basic concept of Quasi-Phase-Matching in a JTWPA. First simulations validated this concept and achieved a gain of more than 20 dB for N = 500…1000 SQUIDs. This concept must be examined more carefully by circuit simulations and circuit parameters must be optimised to attain a smooth frequency dependence of the power gain, before it will be tested in experiments.

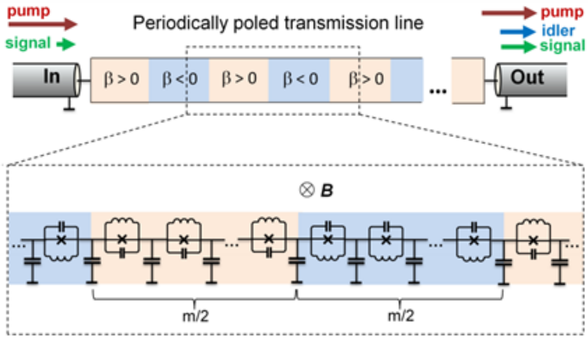

Fig. 5: *Concept of Quasi-Phase-Matching in a JTWPA.*

4.1.2 Physical layout of JTWPA circuits

The rf-SQUIDs of the JTWPA are embedded in a coplanar waveguide (CPW) with an impedance of 50 Ω. Inductors are realised by small meander lines. Capacitors are realised as interdigital structures or as plate capacitors with deposited dielectrics. Using substrate materials with low rf losses, interdigital capacitors are preferred because they are expected to have smaller losses compared with plate capacitors. Unfortunately, it might be difficult to realise large capacitor values with interdigital structures due to space limitations. Layouts for a set of circuit parameters must be adapted according to the envisaged fabrication technology (Nb or Al). Fig. 6 shows a layout developed for the PTB niobium technology.

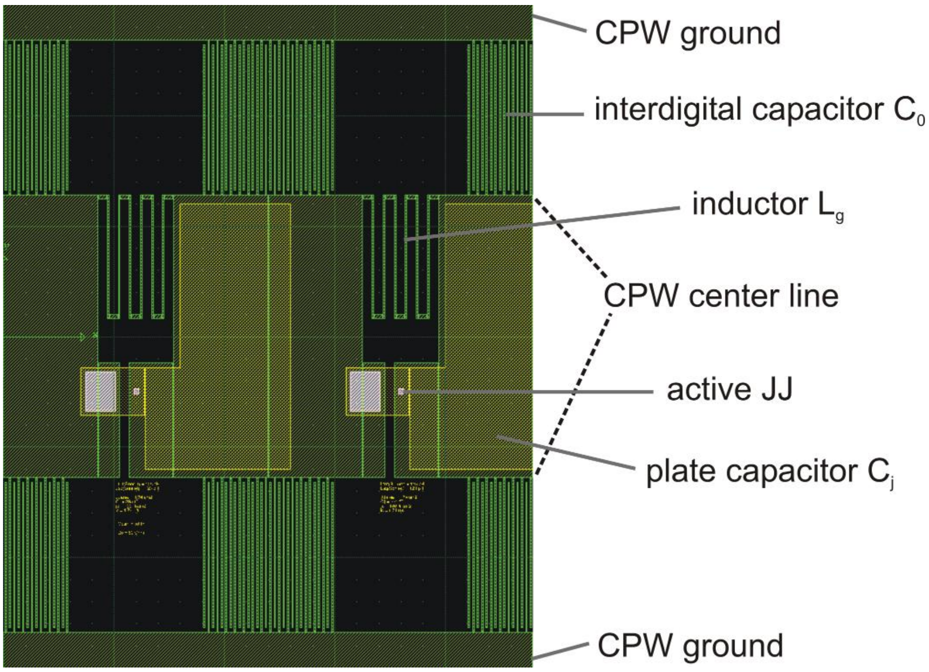

Fig. 6: *Layout of the basic rf-SQUID with interdigital ground capacitors, meander inductors, and increased C_j by adding a shunting plate capacitor in parallel to the small active Josephson junctions for the PTB niobium technology.*

NPL developed several quasi-phase-matched designs based on the theoretical outline given in [10]. The design parameters where simulated (coupled mode equations) and modelled (WRSPICE, SONNET). Lithography masks were made for both an optical and electron beam lithography process. Although fabrication delays where incurred due to the COVID pandemic, several quasi-phase-matched amplifiers have been fabricated at the SUPERFAB facility at RHUL using Al/AlO_x/Al double angle Josephson junction technology and await measurement and characterisation at low temperature. An example mask design and fabricated device are shown in Fig. 7.

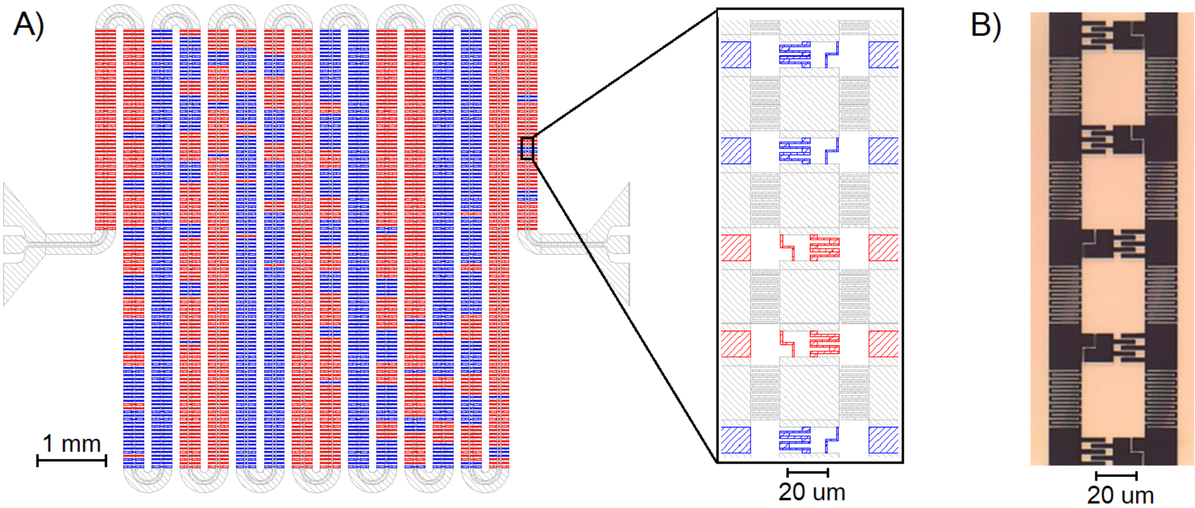

Fig. 7: *(A) Quasi-phase-matched RF SQUID JTWPA electron beam lithography mask design - Junction position colour coded (red/blue). (B) Optical microscope image of this design fabricated at RHUL SUPERFAB using aluminium technology.*

4.1.3 Fabrication technology

JTWPA circuits are fabricated in niobium trilayer technology as well as in aluminium shadow evaporation technology. In the PTB Nb-technology the Nb-layers are deposited by sputtering, while the SiO_2-layer is created by plasma enhanced chemical vapour deposition (PECVD). Both layers are structured by reactive ion etching (RIE) [11]. Plate capacitors can be realised with an SiO_2 insulator layer or with other low loss dielectric material, e. g. Si_3N_4. Since more than 1000 capacitors are needed, a low defect density of the insulator layer is required to avoid shorts in plate capacitors. Chemical-mechanical polishing (CMP) might be used to planarize the insulator layer, but it was found that circuits fabricated without planarization showed a smaller number of defects. The patterns in all layers are usually defined by electron-beam lithography (EBL) using either negative or positive resists. Fig. 8 shows the layer structure for a Nb based Josephson junction and plate capacitor together with a photo of a fabricated Nb sample with interdigital capacitors.

In the LanU Al-technology, the JTWPA chips were fabricated with a multistep process using electron beam lithography. First, the ground plane and bottom electrodes of the JJ shunting capacitors were formed in the Al layer. Then, an insulating layer was formed on top of the ground plane and bottom electrodes either by UV assisted oxidation of Al or by atomic layer deposition (ALD) of Al_2O_3. In both cases the target oxide thickness was 20 nm. Finally, the fabrication of the JTWPA was completed by placing the rf-SQUIDs in the slot of the ground plane, which formed the central electrode of the transmission line. It was found that some of the ground capacitors with the UV assisted oxide layer are leaky resulting in the extremely poor transmission of the microwave signals through the chip. Hence, it was concluded that this process is unsuitable for making this type of parametric amplifiers and the focus was shifted to the JTWPAs made with the ALD process. This process has to be optimised in order to find a good balance between low defect density and reasonably high capacitance per unit area.

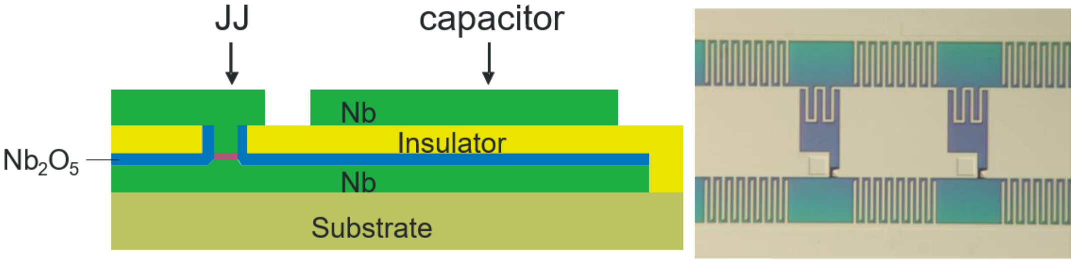

Fig. 8: *Schematic cross section of PTB Nb-technology and photo of a fabricated Nb sample showing interdigital ground capacitors.*

Within the RMG INRIM and NPL created designs optimised for the INRIM aluminium fabrication process based on the Resonant-Phase Matching approach. Several samples have been fabricated at INRIM and tested at NPL.

4.1.4 Summary

The project has investigated in detail the design and layout of a JTWPA with Three-Wave Mixing. Circuit parameters have been optimized and extensive simulations have been performed to analyse the JTWPA behaviour and to examine the effects of parameter spread and defects. Three different approaches for dispersion engineering and phase matching have been explored. The fabrication technologies have been improved and test samples were fabricated in niobium and aluminium technology.
The results clearly demonstrate that it should be possible to create a high performance Three-Wave-Mixing JTWPA based on the available state of the art fabrication technology and achieving the targeted high gain in a wide bandwidth.
Objective 1 has been almost completely achieved. Unfortunately, it was not possible to validate the simulation results experimentally since no defect free devices could be verified before the end of the project due to multiple delays in the fabrication resulting from the COVID pandemic.

4.2 Characterisation of amplifier devices (including noise)

4.2.1 Pre-characterisation setup for Nb devices at 4.2 K

NPL and PTB have set up 4.2 K dip probes for a first quick characterisation of niobium-based devices. Fig. 9 shows a JTWPA sample mounted to the PCB/probe of the NPL setup. The probe allows measurement of up to two 2-port devices at once (4 coaxial rf lines). A simple superconducting coil (~1500 turns) is integrated in the probe over the centre point of the device-under-test (DUT). Finally, a silicon diode thermometer is attached to the cold finger of the probe to monitor system temperature.

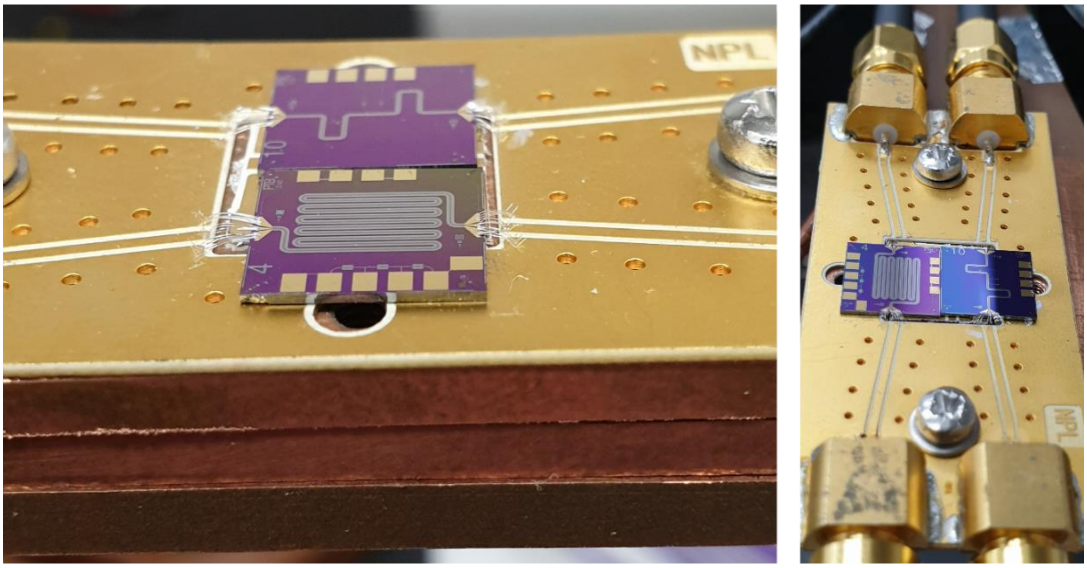

Fig. 9: *PCB with PTB JTWPA and resonator device shown on NPL 4.2 K dip probe. Magnet and thermometer not shown.*

A flux-biased measurement scheme as shown in Fig. 10 was used at NPL to characterise the JTWPA samples. The signal and pump are provided by two Microwave Generators. The output of the JTWPA is measured using a Spectrum Analyser. The whole measurement is referenced according to the 10 MHz clock out of the spectrum analyser.

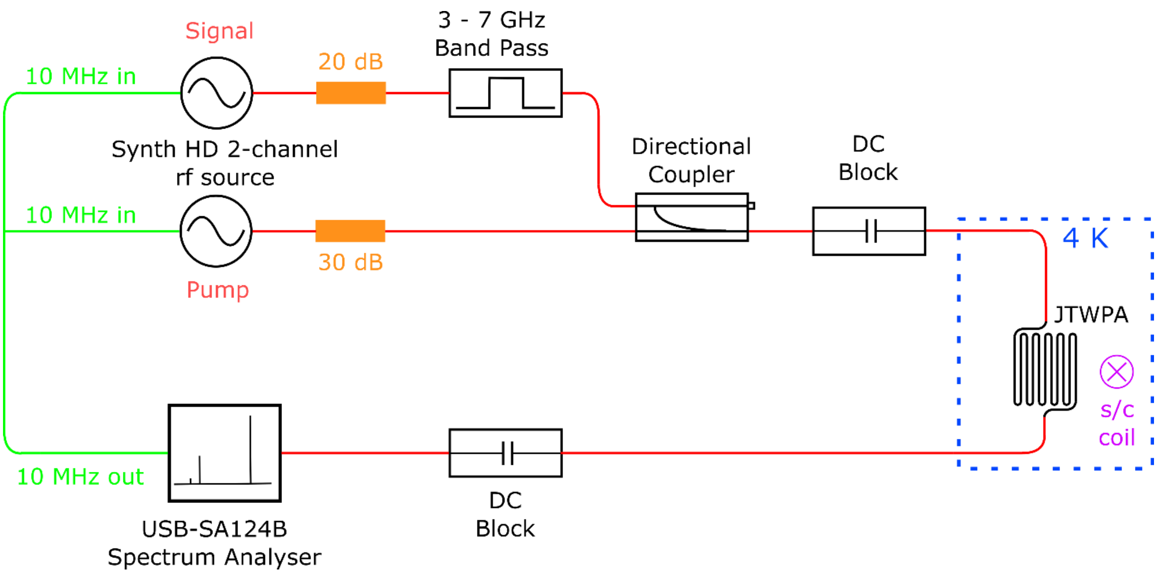

Fig. 10: *Schematic of NPL 4 K flux-biased measurement platform. The "measurement" circuit is shown in red. The "timing" circuit is shown in green. The JTWPA and the superconducting coil are held at 4.2 K in a dip probe.*

Fig. 11 shows an example of a flux-biased measurement of a Niobium based JTWPA prototype sample. The flux bias was tuned at each frequency to give the maximum gain. The gain drops from 9 dB to about 3.5-5 dB in the examined frequency range from 5.5 GHz up to 6.5 GHz.

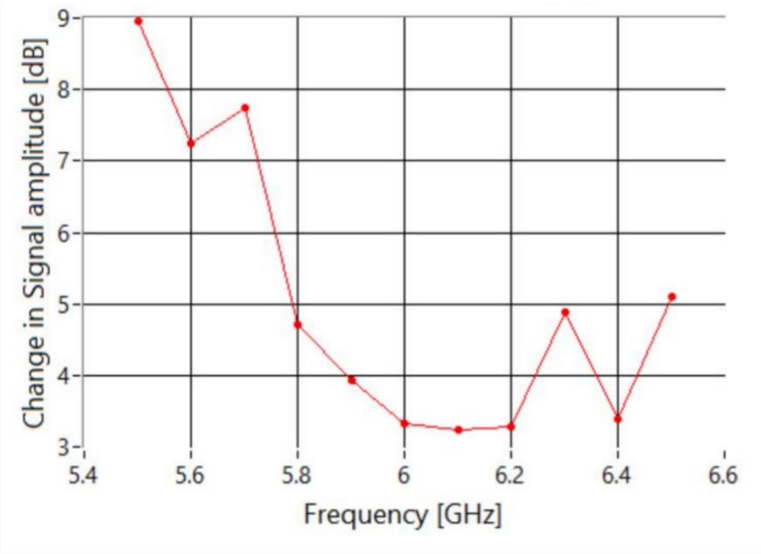

Fig. 11: *Gain of a Nb JTWPA prototype shown in the frequency range 5.5-6.5 GHz where the flux bias is tuned at each point to give highest gain, recorded with the NPL 4.2 K flux-biased measurement platform.*

4.2.2 Rapid test facility operating at 300 mK

NPL has constructed a complete quantum amplifier metrology system with a base temperature of 300 mK for rapid screening and testing of devices fabricated in aluminium or niobium technology.
A full characterisation of an amplifier requires a multi-dimensional sweep of several parameters including frequency and power of the signal and pump tones together with dc bias settings. Software was developed at NPL specifically for this purpose to enable the measurement sequences to be specified and then the data analysed by making cuts across various planes defined by parameters. More details of this system and the software are given in section 4.3 below together with an example measurement on a device fabricated at PTB.

A commercially available variable temperature noise source, of a special design to operate at cryogenic temperatures, was purchased for integration into either the 300 mK test facility or a dilution refrigerator operating below 30 mK. The source can easily be transferred from one system to another. The noise source has a through coaxial transmission line so that noise can be added to an existing microwave signal. A photograph of the source is shown in Fig. 12.

Several prototype amplifier devices from project partners were measured at 300 mK in the rapid test facility at NPL. Samples have been characterised in terms of bandwidth, gain and their output spectrum. Feedback was given on the need for an appropriate modification of the dispersion within the JTWPA to avoid the creation of strong higher order mixing products and second harmonic generation, limiting the achievable gain. The results of the sample characterisations also helped to improve the device layout and the fabrication technology.

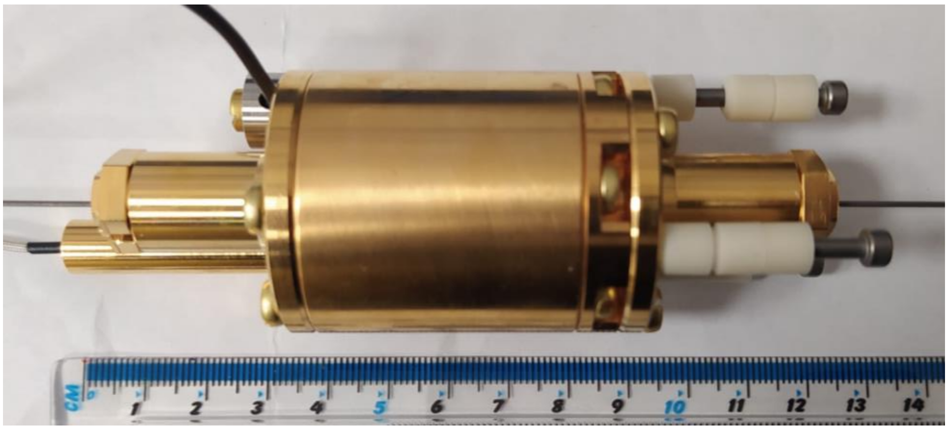

Fig. 12: *Photograph of the cryogenic noise source showing the input and output coaxial lines on the left- and right-hand sides.*

4.2.3 Dilution refrigerator setup for characterisations at about 20 mK including noise measurements

A low-temperature (dilution cryostat) setup at RHUL is operational for the characterisation of both resonator and travelling wave parametric amplifier devices at the many photon level at about 25 mK temperature. This setup with a bandwidth of 4 to 8 GHz is optimised for noise squeezing experiments and measurements at the quantum limit. Microwave equipment to support noise squeezing measurements is available for deployment on the low temperature measurement system when suitable parametric amplifier devices become available.

A further low-temperature measurement setup at PTB, also based on a dilution refrigerator, has been completed with the aim of characterising the JTWPA circuits from objective 1 at a temperature of about 20 mK with a focus on their linearity, dynamic range, and noise, using standard microwave generators and thermal noise sources. Photos and the measurement scheme are shown in Fig. 13.

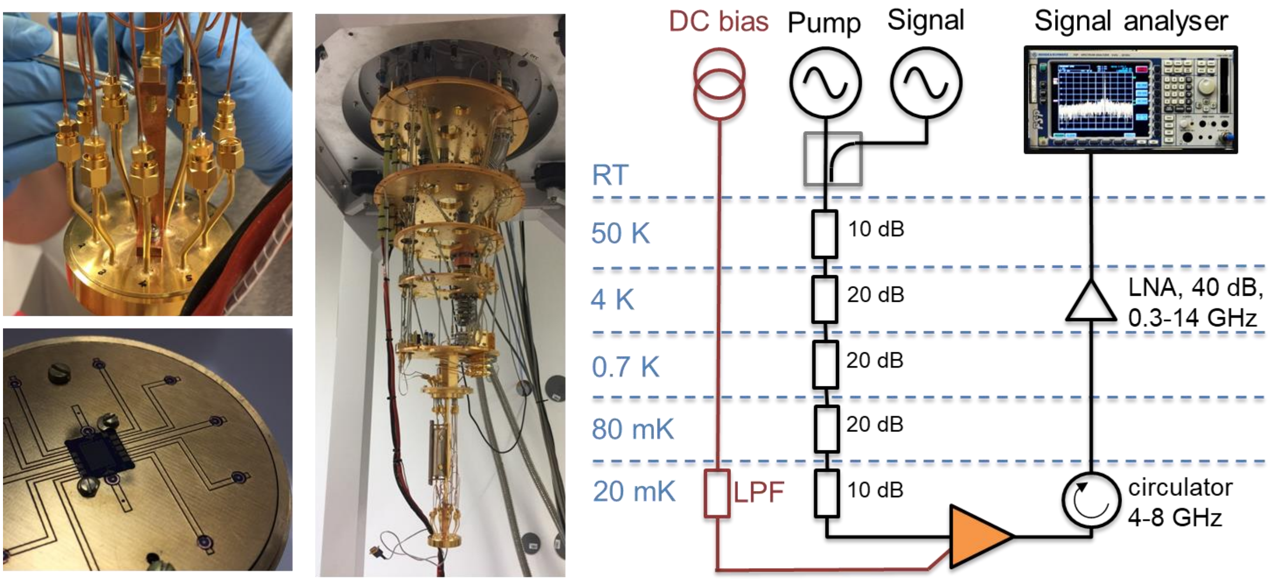

Fig. 13: *Photos of the PTB dilution refrigerator and the schematic measurement setup*.

Unfortunately, no defect free samples with sufficiently good properties could be selected for the noise measurements and demonstration of thermal noise-squeezing before the end of the project.

4.2.4 Summary

The project has characterised several JTWPA samples fabricated in Al and Nb technology. Samples have been characterised in terms of bandwidth, gain and their output spectrum. Feedback was given to improve the device layout, the fabrication technology and the need for a customised dispersion. The project has optimised the device parameters regarding a modified dispersion relation and to obtain a good signal gain, large bandwidth, and high dynamic range of the amplifiers.
Objective 2 was only partially achieved. It was not possible to complete the planned final noise measurements, because no defect free samples with sufficient gain could be verified before the end of the project due to multiple delays in fabrication of devices resulting from the COVID pandemic. It is anticipated that measurements will be carried out after the end of the ParaWave project within several follow-on projects.

4.3 Quantum amplifier metrology

Metrological characterisation of parametric amplifiers based on superconducting technology requires both a low temperature environment to realise the full performance of the superconducting materials and traceable radio frequency (RF) equipment operating in the GHz range for the determination of key parameters including gain, bandwidth, and noise performance.

The ultimate noise performance of a parametric amplifier can only be demonstrated at a temperature of 30 mK or below. However, all other parameters can be measured at a temperature of 300 mK which is much easier to realise. NPL therefore specified and constructed a complete quantum amplifier metrology system with a base temperature of 300 mK for rapid screening and testing of devices fabricated in aluminium or niobium technology by the project partners. Devices with good performance could then be further evaluated at 30 mK in a dilution refrigerator.

4.3.1 Low temperature system

A photograph of the 300 mK system in the NPL laboratory is shown in Fig. 14. The main cryostat vacuum enclosure can easily be lowered to access the parametric amplifier samples. Cooling to a temperature of 2.5 K is provided by the pulse-tube machine on top of the cryostat with lower temperatures realised by the circulation of ^{4}He gas to provide a stage at 1.2 K and ^{3}He gas to provide the base temperature at 300 mK. The circulation gases are stored in the two yellow cylinders in the right of the figure when not in use. The whole system is computer-controlled and is able to provide continuous operation at the base temperature for extended characterisation of amplifier devices.

Fig. 14: *Photograph of the 300 mK system established for parametric amplifier metrology, the cryostat and cooling system was supplied by the ICE Oxford company in the UK*.

4.3.2 Cryogenic wiring and sample environment

The parametric amplifiers are typically fabricated on a chip size of 10 mm by 10 mm. Coaxial electrical connections at the amplifier input and output suitable for GHz frequencies are required and, according to design, some further connections for direct current (dc) bias and control. The chip also needs to have good thermal contact to the refrigerator to ensure that the base temperature is achieved at the device. Overall electrical screening is required to ensure that a well-controlled RF circuit is achieved as well as the lowest noise levels.

To meet these requirements, sample enclosures were designed and specified for manufacture by the Aivon company in Finland. An example is shown in Fig. 15. Connections to the chip are realised using wire bonds to the surrounding printed circuit board (PCB).

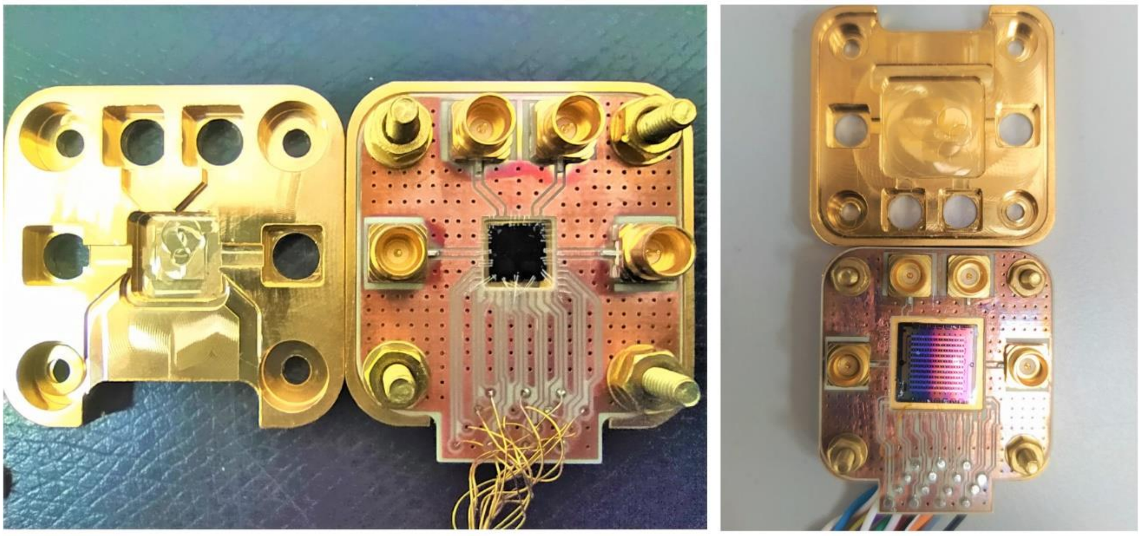

Fig. 15: *Examples of the screened enclosure developed for parametric amplifier samples. Four coaxial connectors are provided around the perimeter together with a number of dc connections via individual wires. Models for two different chip sizes are illustrated*.

In order to carry out measurements of the amplifier samples at low temperature, specialised connections for RF power and dc bias from the instruments located at room temperature are required. These connections have to maximise electrical performance and minimise thermal heat flow from room temperature to the low temperature stages where the cooling power is limited. At the same time, the coupling of electrical noise from room temperature to the amplifiers has to be kept at a minimum level. Fig. 16 shows a schematic of the wiring scheme developed to meet these requirements. The figure illustrates three RF lines for supplying power and test signals to the amplifier input as well as an RF line for returning the amplified signal to room temperature. The dc bias lines are also shown. Each of the input lines is thermally anchored at three cryogenic temperatures to control the heat flow and reduce thermal noise coupled to the device under test. A cryogenic amplifier is installed in the output RF line to obtain the best signal-to-noise ratio for the experiments. The installation includes cryogenic RF coaxial switches so that different amplifiers can be selected in one experiment together with calibration circuits for standardisation of the gain measurements.

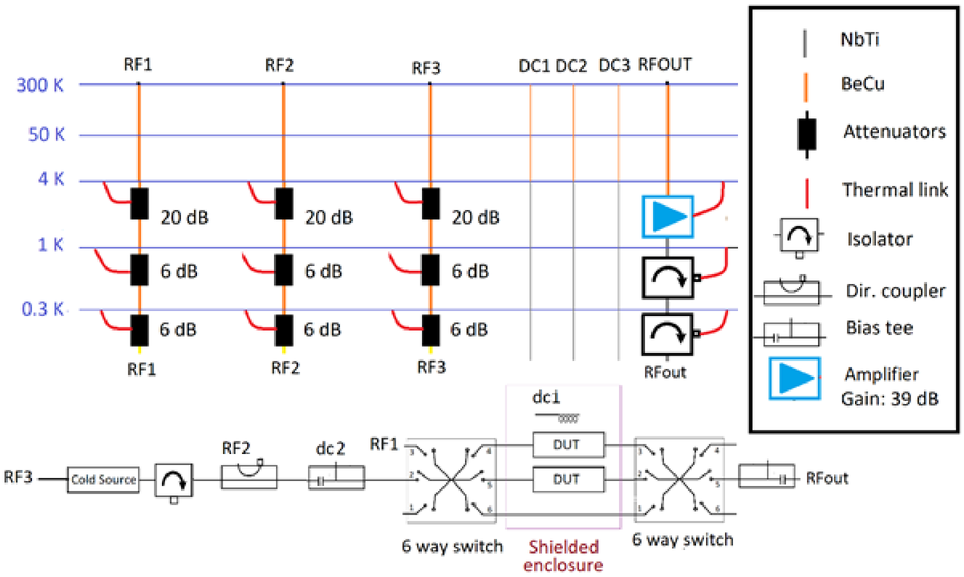

Fig. 16: *Schematic diagram of the wiring for RF and dc connections inside the cryostat. The detail for the switching of different samples and calibration lines is also shown, together with the 'cold source' which can provide calibrated levels of noise using a scale of known internal temperatures and a fixed impedance*.

For some designs of parametric amplifier, an external, adjustable magnetic field is required to bias the RF-SQUID devices to the correct operating point. A practical amplifier with many amplification cells can occupy an area of up to 1 cm^2 and it is necessary to provide a magnetic field which is uniform over this area to a few percent. A pair of Helmholtz coils was designed for the cryogenic measurement environment and the coils and sample are surrounded by a low temperature, high-permeability magnetic shield to screen background field from the Earth's magnetic field and magnetised objects in the laboratory. Fig. 17 shows an engineering drawing of the coils and calculations of the field density and uniformity.

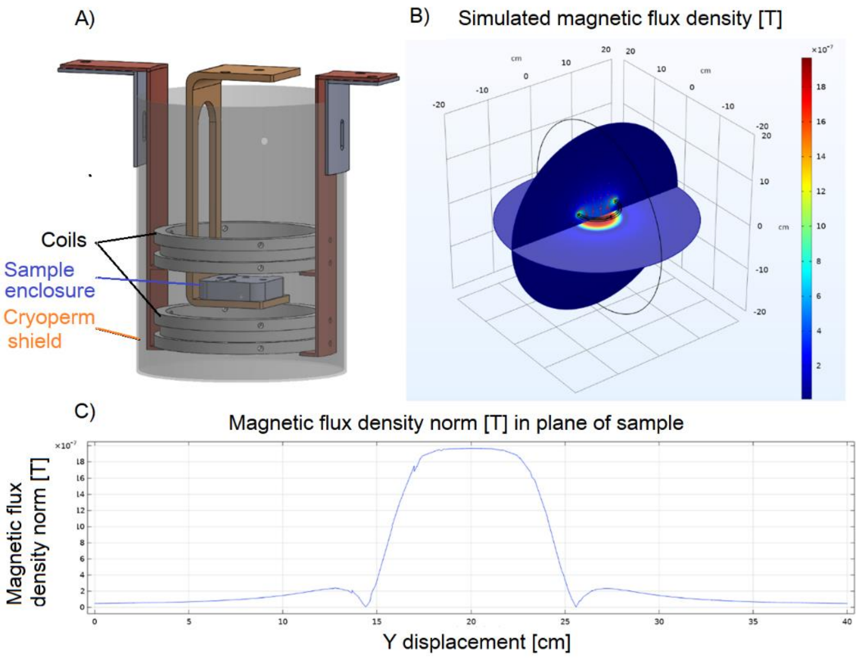

Fig. 17: *Engineering drawing for the Helmholtz coils and calculations of the magnetic field density and uniformity in the plane of the parametric amplifier device*.

4.3.3 Measurement instrumentation and software

The instrumentation located at room temperature for metrological measurements comprises RF signal sources, spectrum analysers and network analysers. A typical characterisation of a parametric amplifier requires measurements at many individual frequencies and RF power levels, automation of the data collection is therefore essential. Measurement software was specially developed for this purpose and facilitates frequency and power sweeps of different parameters in different instruments through a simple user interface panel. A screenshot of the user interface is shown in Fig. 18. Large volumes of data are created during a measurement sequence so further software is also required to analyse the data and present summary graphs to the user. Again, computer software was specially created for this purpose and an example screenshot is shown in Fig. 19.

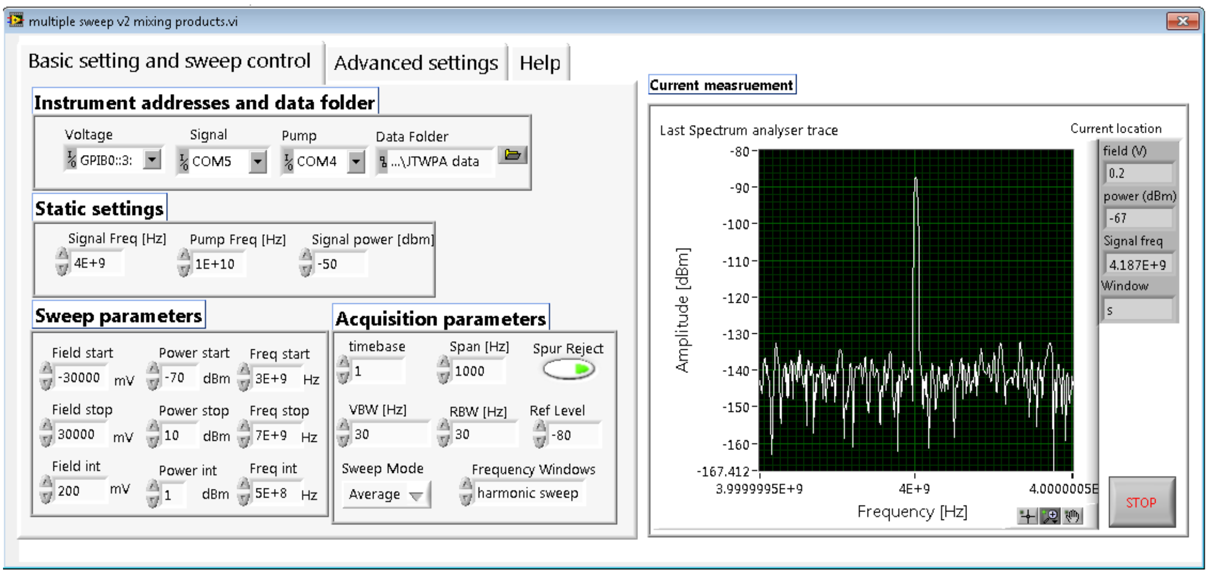

Fig. 18: *Example screen capture of the measurement software showing a typical measurement from a parametric amplifier characterisation*.

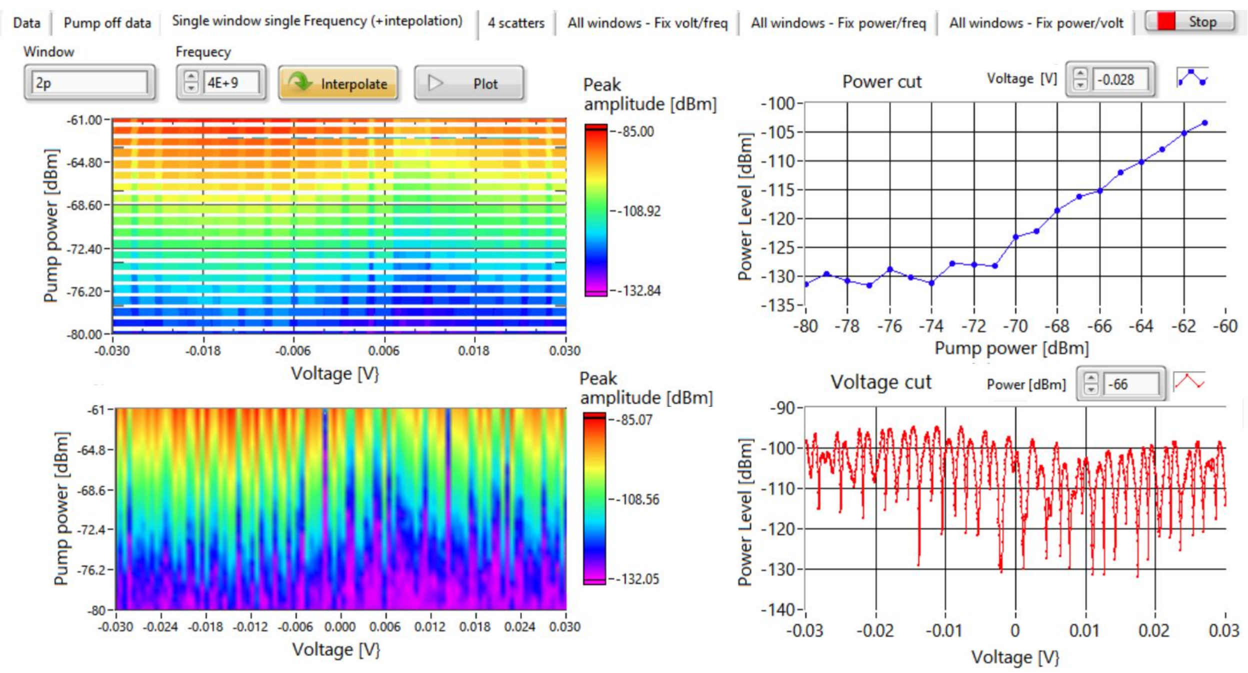

Fig. 19: *Example screen capture of the data analysis software showing results from a parametric amplifier operating with a 10 GHz pump wave and a 4 GHz signal tone. (Left) Measured amplitude of the second harmonic of the pump tone (2p) generated at the output of the amplifier is plotted as a function of pump power and voltage (top: raw data, bottom: interpolation). (Right) Cuts are made in the data set at various points in power (top) and voltage (bottom). The periodic dependant of the SQUID based amplifier is on the current bias is clearly apparent from the voltage cut displayed*.

4.3.4 Summary

A bespoke cryogenic measurement system was specially constructed and configured for metrological characterisation of parametric amplifiers including the development of computer software for data collection and analysis. Traceable measurement of amplifier parameters is assured by using calibrated instruments at room temperature in combination with reference calibration lines at low temperature and a variable-temperature cryogenic noise source. The system was used to characterise a number of devices fabricated by partners during the project.

Objective 3 has been completely achieved.

4.4 JTWPA integration with quantum sensors

4.4.1 rf-SET

Solid-state quantum sensors operate at low temperatures and hence require a cold environment which is usually provided by some sort of a cryostat. A particular example of a quantum sensor is a Cooper pair transistor, which is a three-terminal device consisting of a small island tunnel coupled to the source and drain electrodes. The island potential is controlled by a capacitively coupled gate electrode. The device operation temperature is determined by two characteristic energies: the charging energy E_c and the Josephson energy E_J. For the optimal device operation both energies must be comparable, $E_c \approx E_J$. Another requirement for the device operation is that the tunnel junction resistance must exceed the resistance quantum $R_Q \approx 6.5$ kΩ. With a commonly used material, aluminium, which is a superconductor that forms a high-quality oxide layer used as a tunnel barrier, the operation temperature of the Cooper pair transistor is in the mK temperature range. This dictates the use of a dilution refrigerator as a main cryogenic tool.
Characterisation of Copper pair transistors as ultrasensitive charge detectors is usually done with room temperature electronics. With heavily filtered DC measurement lines having the stray capacitance of ~ 10 – 100 nF and the output impedance of ~ 10 kΩ, the characteristic time constant of the measurement setup appears to be ~0.1 – 1 ms. This limits the measurement bandwidth of charge detectors to below 10 kHz. Another issue is the separation between the sensor and the first-stage amplifier. The fact that they are at least 2 m apart introduces noise, thus deteriorating device sensitivity. Bringing a high-frequency amplifier closer to the sensor will kill two birds with one shot: the device sensitivity will improve and so will the bandwidth.
An ideal candidate for the low temperature low-noise amplifier is the Josephson travelling wave parametric amplifier (JTWPA) developed as part of the ParaWave project. A typical JTWPA is designed to operate in the GHz frequency range with the wave impedance of 50 Ω, hence it has this impedance at both the input and output ports. The impedance of quantum sensors varies a lot, from very low (Ω's) for SQUIDs to very high (tens and hundreds of kΩ or even MΩ) for single-electron transistors. The fact that the sensor (source) impedance differs a lot from the amplifier (load) impedance leads to signal reflection which causes destructive interference creating standing waves in the measurement chain. As a result, power transfer degrades. This fact causes significant difficulties in using JTWPAs as a first stage of the amplification cascade for quantum sensors. Thus, a matching scheme becomes an essential interface between sensors and JTWPA.
The role of the matching scheme is to minimize signal reflection and maximize power transfer by using extra elements to match source and load impedances. In this project we have considered the possibility of the microwave readout of a high-ohmic sensor, a Cooper-pair transistor with a characteristic impedance of about 10 kΩ. A similar approach can be applied to other types of sensors, such as an SIN thermometer with a higher impedance or a SQUID with a lower impedance. The operation frequency range of JTWPAs' does not allow us to use lumped element matching circuits. To solve this problem, we designed and fabricated the matching schemes based on the distributed microwave components. Two types of matching schemes were considered as described below.

1. Stub matching scheme

Stubs are often used to match a load impedance to the transmission line characteristic impedance (50 Ω in our case) due to their simplicity. A stub is a part of the transmission line that is connected at one end only. The free end of the stub is either left open-circuit or short-circuited. The other end of the stub is connected to the main transmission line adding either capacitive or inductive load depending on the stub length. The stub is positioned at a certain distance from the load, which is chosen so that at that point the resistive part of the load impedance is made equal to the resistive part of the characteristic impedance. This is called impedance transformation and occurs due to the action of the length of the main line. The length of the stub is chosen so that it exactly cancels the reactive part of the presented impedance. That is, the stub is made capacitive or inductive according to whether the main line is presenting an inductive or capacitive impedance, respectively. Stubs thus function as capacitors or inductors at microwave frequencies and their behaviour is due to standing waves along their length. The length of the stubs depends on the frequency used; at GHz frequencies the wavelengths are short enough that the stub is conveniently small as compared to the RF frequency range. A single stub will only achieve a perfect match at one specific frequency. For wideband matching several stubs may be used spaced along the main transmission line.
To design the stub matching scheme, it was first necessary to decide what geometry to use: whether the stub should be a series or parallel stub. Then it was necessary to decide whether the stubs should be shorted or open-ended. The design should allow measurements of *S* parameters of the circuit (mainly the reflection coefficient) as well as a 4-point measurement of the device under test (a Cooper pair transistor or a single junction). In particular, it was important to take transport measurements such that wire bonds would not affect

the microwave circuit characteristics. It was concluded that the only reasonably possible solution was using symmetric parallel shorted stubs. Furthermore, the shorted stub design had smaller dimensions. The high-ohmic sensor, i.e., the SIN junction, has been created on the top of a thin insulating layer, this allowed to short the stubs for a high-frequency signal but not for a DC signal by effectively creating a low pass filter at the end of each stub due to the capacitance between the ground plane and the stub top layer.
An optical image of the chip containing the stub matching scheme is shown in Fig. 20. The whole structure was fabricated by multistep electron-beam lithography. The main transmission line runs through the chip from left to right and is surrounded by four auxiliary structures, i.e., single junctions used for tests. The two stubs are located next to the RF bonding pad and are connected to the transmission line at one end and shorted to ground at the other end. The blue background corresponds to the ground plane covering the entire chip. The ground plane has several windows (green) where the ground plan is removed, allowing test structures and bonding pads to be deposited (yellow). The low-pass filter structures can be seen as large yellow rectangular areas joining each of the DC bonding areas. The end of each rectangular area is a bonding pad. There is a small region indicated by the arrow where a single junction is located.

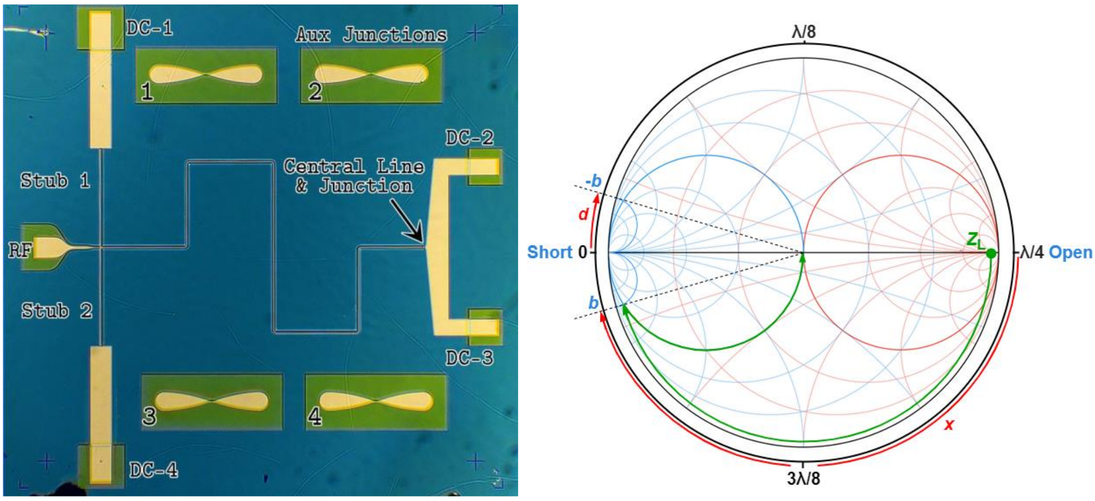

Fig. 20: *(Left) Polarised filter photo of the full chip (chip size is about 5 mmx5 mm) after metallisation. This was a good chip with no clear defects upon closer optical examination. Green is gap in the ground plane (blue) with the metal layers visible in yellow. Stub 1 and Stub 2 are the matching stubs shorted to the ground plane through large capacitances; DC-1(2,3,4) are contact pads for DC measurements; RF is the contact pad for the microwave input/output; 1(2,3,4) are auxiliary structures for test measurements.*

(Right) Smith chart diagram indicating how the transmission line of length x and shorted stub of length d is used to match the load impedance of Z_L = 10 kΩ to 50 Ω.

2. Quarter-wave impedance transformer

A quarter-wave impedance transformer (QWT) is a transmission line of length λ/4, where λ is the wavelength at a particular frequency, terminated with some known impedance (device impedance). In microwave engineering, it does the same job as a stub, however, whereas a stub is terminated in a short or open circuit and the length is chosen to produce the required impedance, the λ/4 transformer is the other way around: it always has a length of λ/4, hence the name, and the termination is designed to produce the required impedance.
In the present project, the transmission line was implemented as a coplanar waveguide (CWG) which was fabricated using printed circuit board technology. The primary concern with the QWT was its inherent size due to the scale of the wavelengths being used, which, as will be discussed, explains why a PCB was used instead of fabricating the QWT on the same chip with the device under test. In order to match the 10 kΩ load to the 50 Ω at f ~ 4.5GHz, a quarter wavelength CWG of impedance Z_{QWT} ~ 700 Ω should be used. Such impedance is greater than the impedance of free space ~ 377 Ω, thus a multi-QWT approach was required. The following expression allows the estimation of the length of a QWT based upon the parameters of the medium and frequency:

$$\ell_{QWT} = \frac{\lambda}{4} = \frac{c}{4f}\frac{1}{\sqrt{\varepsilon\mu}},$$

where the relative permeability $\mu \sim 1$ and the relative permittivity ε is determined by the material and *c* is the speed of light.

For a silicon-based microchip ($\varepsilon \approx 11.7$), the QWT length would be $\ell_{QWT} \approx$ 4.87 mm which would be incredibly difficult to fit onto a chip which has dimensions about 4.5 mm × 4.5 mm, requiring much greater complexity in geometry increasing the risk of error/damage during development and also removing space which could be filled with auxiliary junctions (like in the stub scheme) which improve the chance of a successful junction being developed. Thus, it was decided that a PCB would be used as the size constraint on this medium was simply the dimensions to allow it to be mounted into the dilution refrigerator. This was estimated to be 100 mm × 50 mm, although this was a limit and not a target, ideally, the board would be as small as possible.

The PCB in question was a “Rogers RO3010 TM” laminate, with $\varepsilon_r = 10.2 \pm 0.3$ which gives an approximate $\ell_{QWT} \approx 5.22$ mm, well within the board's size constraints.

There were, however, limitations to the QWT itself caused by the precision of the board milling machine of 0.2 mm, the wavelength itself which limits the track width to $\lambda/4$, and finally the potential for shorts. The milling precision and QWT conductor track width were relatively insignificant restrictions to overcome, however, the potential for shorts was a major obstacle. In any one QWT section, the conductor track width W could be no greater than W + 2G (where G is the gap width) of a neighbouring QWT section as this would cause the central track to short out. Based upon these restrictions the impedance ranges available to use were from15 Ω to 60 Ω. Due to the explained restrictions, an alternating pattern was designed. The load is first transformed to a low impedance, which is then transformed to a high impedance (lower than the load), with this process repeated until Z_0 = 50 Ω is met.

The fabricated PCB with a QWT is shown in Fig. 21. The QWT allows to match 10 kΩ load to 50 Ω at a frequency of 4.5 GHz in the bandwidth of 1 GHz.

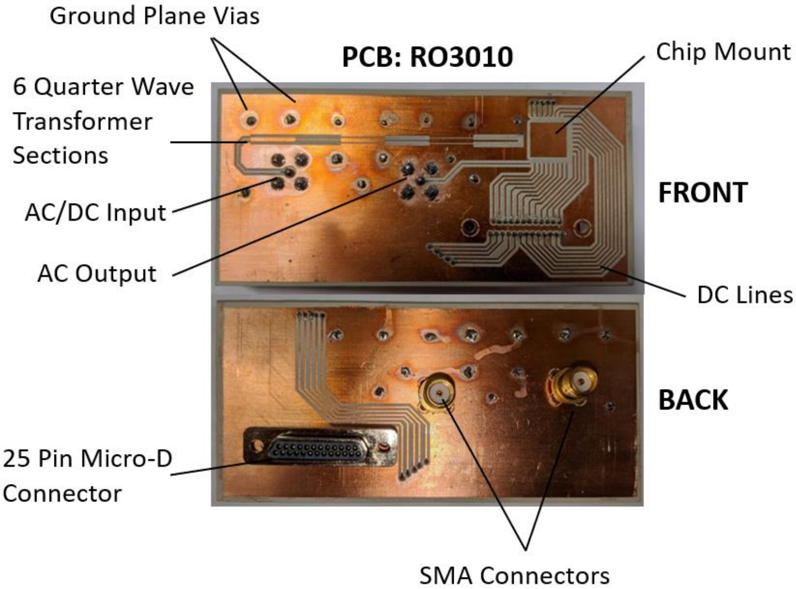

Fig. 21: *A PCB containing all necessary elements as labelled in the top and bottom images, including a multi quarter wave transformer shown in the top image.*

4.4.2 nanoSQUID

The objective of this work was to fabricate nano-scale SQUIDs and to improve the noise performance of the readout circuits by integration with a parametric amplifier. SQUIDs were developed in both niobium and aluminium technology.

At PTB, nanoSQUIDs were fabricated using overdamped superconductor-normal metal-superconductor (SNS) trilayer Nb/HfTi/Nb Josephson junctions. A combination of electron-beam lithography with chemical-mechanical polishing (CMP) and magnetron sputtering on thermally oxidized Si wafers was used to produce nanoSQUIDs with down to 100 nm lateral dimensions for Nb lines and junctions. Fig. 22 shows an example of a three-axis vector magnetometer, which achieved a flux noise below 250 n$\Phi_0/\sqrt{\text{Hz}}$ in the white noise regime

[12]. All three nanoSQUIDs can be operated simultaneously and their signals can be frequency multiplexed and amplified by the JTWPA as a first-stage amplifier in a future modified version of this device.
Details of the fabrication process including an extension from originally two to three independent Nb layers have been published in [13].

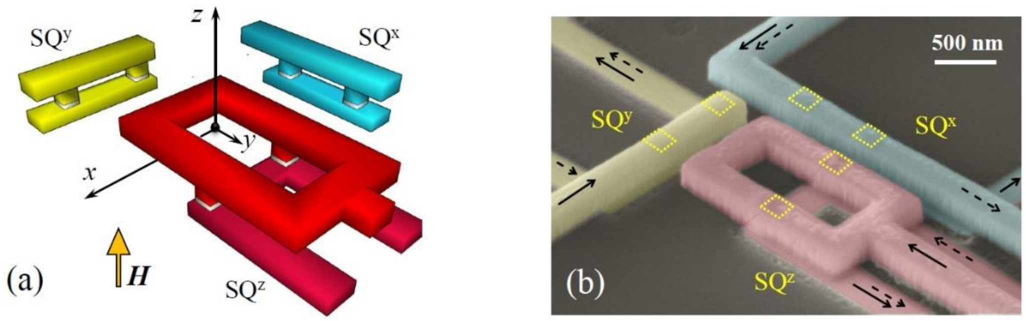

Fig. 22: *(a) Schematic representation of the three-axis vector nanoSQUID; (b) False-coloured SEM image of a typical device. Yellow dashed squares indicate the position of the Josephson junctions*.

At NPL and RHUL, SQUIDs with µm-scale junctions were fabricated in aluminium technology using a double-angle shadow evaporation technique. Two aluminium layers are deposited with an oxidation step in between. A Dolan bridge created in the photoresist creates a shadow when the sample is titled enabling two overlapping areas to be deposited. The aluminium oxide Josephson junction is combined with an inductor to make a SQUID. A single junction and an inductor in series forms an 'RF-SQUID' for bias and measurement at radio frequencies. Alternatively, two junctions can be connected in parallel to form a 'DC-SQUID' which is normally operated with a direct current bias. Fig. 23 shows some example devices imaged using a scanning electron microscope.

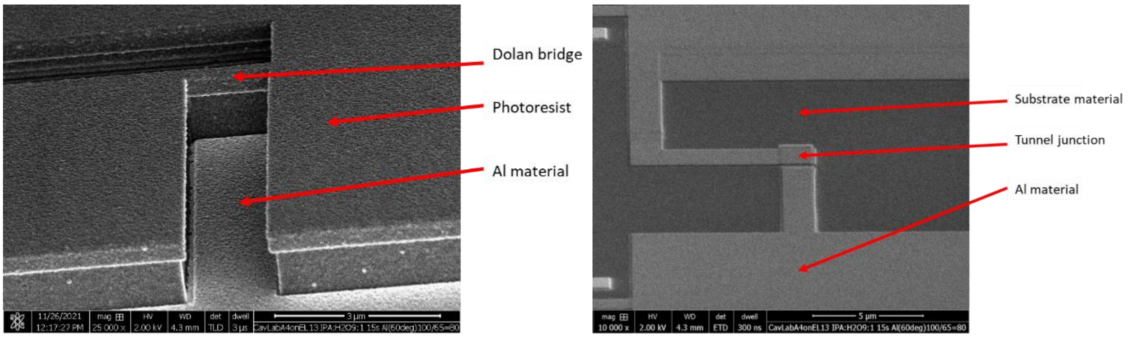

Fig. 23: *(Left) Aluminium – aluminium oxide tunnel junction fabricated using a double-angle evaporation technique. A Dolan bridge in photoresist material suspended over the substrate provides a shadow for the two-step process. (Right) Tunnel junction after excess aluminium material has been removed with the photoresist using a lift-off process. Junction area is approximately 1 µm^2*.

Two options were developed for matching a nanoSQUID to a travelling wave parametric amplifier, one using a bulk resonant circuit and the other using a transmission line resonator. These design options are shown in Fig. 24 and Fig. 25 respectively.

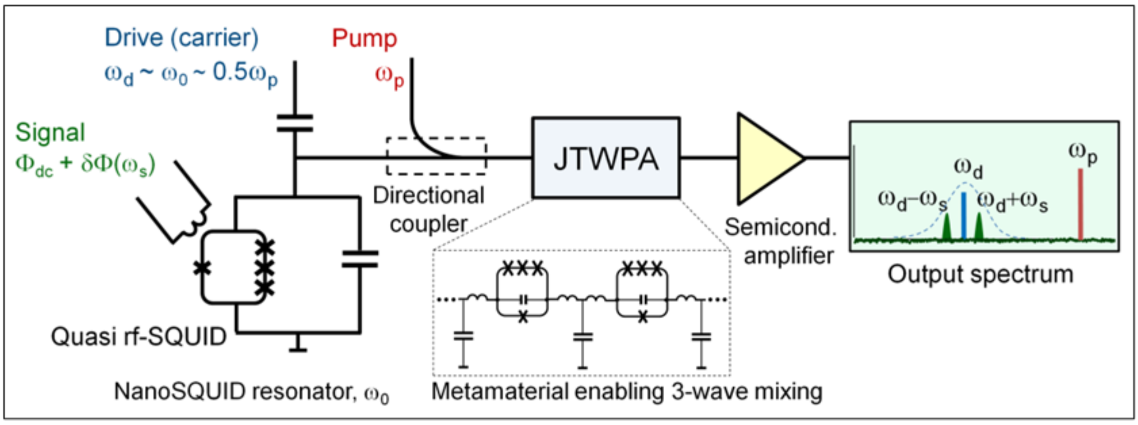

Fig. 24: *Integrated circuit including resonator with nanoSQUID and the Josephson traveling-wave parametric amplifier with three-wave mixing, both based on the same nonlinear elements, i.e., quasi rf-SQUIDs. The quasi rf-SQUIDs can be replaced by ordinary one Josephson junction rf-SQUIDs with geometric inductors. The passive directional coupler can be either a stand-alone component or fabricated on the same chip using a thin-film design.*

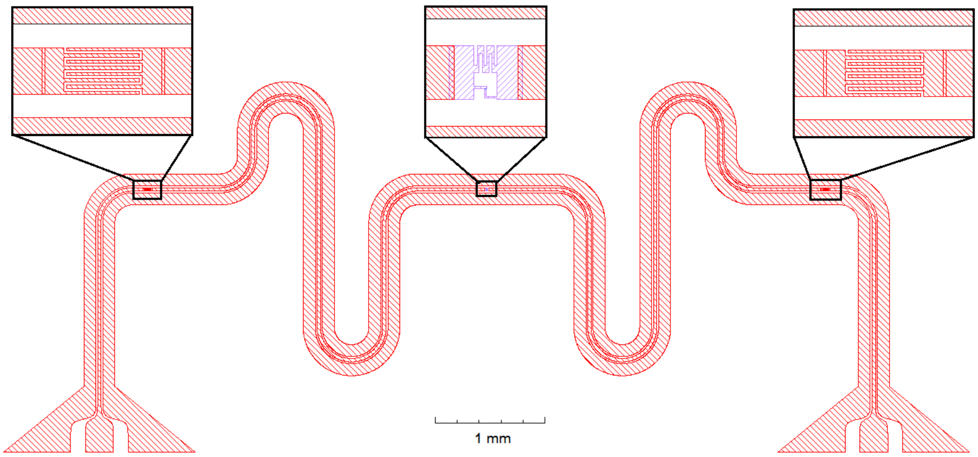

Fig. 25: *Resonator design for readout of a single SQUID sensor at 4 GHz. The SQUID is located at the centre of the resonator where the current is the largest for the fundamental mode. The resonator is weakly coupled to the transmission line at either end using finger capacitors.*

4.4.3 Summary

The project has fabricated and characterised two types of quantum sensors, rf-SET charge detectors and nanoSQUIDs. Several schemes for matching the impedance of the sensors to the 50 Ω JTWPA have been verified and fabricated.
Objective 4 has been achieved to a large extend. Although the quantum sensors and coupling schemes have been finalised, it was not possible to complete the final experimental demonstration of the operation of the sensors together with a JTWPA as a first stage amplifier before the end of the project due to multiple delays in fabrication of devices and laboratory access restrictions resulting from the COVID pandemic.

References

[1] A. B. Zorin, Phys. Rev. Applied 6, 034006 (2016)
[2] A. B. Zorin, Phys. Rev. Applied 12, 044051 (2019)
[3] T. Dixon et al, Phys. Rev. Applied 14, 034058 (2020)
[4] S. Ó Peatáin et al, submitted to Phys. Rev. Applied
[5] C. Macklin et al, Science 350, 307 (2015)
[6] T. C. White et al., Appl. Phys. Lett. 106, 242601 (2015)
[7] C. Kissling et al., submitted to Phys. Rev. Applied
[8] L. Planat et al., Physical Review X 10, 021021 (2020)
[9] V. Gaydamachenko et al., in preparation
[10] A. B. Zorin, Appl. Phys. Lett. 118, 222601 (2021)
[11] R. Dolata et al, J. Appl. Phys. 97, 054501 (2005)
[12] M.J. Martínez-Pérez et al, ACS Nano 10 (2016) 8308-8315
[13] S. Wolter et al., Micromachines 2021, 12(4), 350

5 Impact

The project website has been updated regularly, as well as a ResearchGate Project Webpage. A stakeholder group was formed with more than 30 individual members from universities, research institutions, NMIs and small and large companies located in and outside of Europe. The stakeholder group includes the National Institute of Standards and Technology (NIST, USA), The National Institute of Advanced Industrial Science and Technology (AIST, Japan) and the Institut de radioastronomie millimétrique (IRAM, France).

The consortium has given more than 45 posters and presentations on the results of the project at national and international conferences such as the International Scientific Conference on Superconducting Quantum Technologies, the 14th and 15th European Conference on Applied Superconductivity, EUCAS 2019 and 2021, and the Applied Superconductivity Conference, ASC 2020. In addition, the project has published 12 open access peer-reviewed publications in scientific journals such as Applied Physics Letters, Phys. Rev. Applied, Nature Nanotechnology and IEEE Transactions on Applied Superconductivity.

The project organised an international online workshop on “Superconducting Parametric Amplification” for stakeholders and interested participants. Eight presentations were given by consortium members and five talks by international experts. The project received positive feedback from the participants, and the event stimulated interesting discussions and follow-on projects.

Impact on industrial and other user communities

The project's development of the JTWPA will have a major impact on the field of quantum computing in the long term, it will be of particular interest to high-tech industries (e.g., project stakeholders Google LLC and IBM) who require simultaneous measurement of the states of a large number of qubits. The project’s JTWPA, when integrated with quantum sensors will also allow the amplification of extremely small microwave signals with the lowest possible noise, which is critical for the next generation of cryogenic measurement equipment needed for delicate quantum measurements.

The project produced parametric amplifier designs, external microwave circuits for operating the amplifiers and techniques for interfacing the amplifiers to different quantum-based sensors. It also developed unique cryogenic parametric amplifiers that will be of interest to high-tech companies engaged in quantum computing and the manufacture of ultrasensitive instruments using quantum devices and systems such as Magnicon, Germany and York Instruments Ltd, UK.

Inspired by this project, the SME SeeQC.EU, based in Italy, started its own JTWPA research program. SeeQC.EU is developing the first digital quantum computing platform for global businesses and it presented its first results at the Applied Superconductivity Conference 2018 in Seattle, USA.

Impact on the metrology and scientific communities

Single-photon real-time detection is essential in technologies such as: quantum computing with solid-state circuits and microwave photons; quantum key distribution for secure communication; ultrasensitive spectrum analysis of microwave components; and quantum interference experiments with non-classical photon states (beating the standard quantum limit). The use of the JTWPA in the qubit readout circuits will substantially improve manipulation and characterisation of quantum circuits and facilitate the development of a quantum processor. This project will also advance quantum information processing and communication with microwave frequencies, where high-fidelity detection of single microwave photons is indispensable.

Fundamental and new quantum optical experiments in the microwave regime are of considerable interest to the scientific community. The experiments include, the second harmonic generation, parametric down conversion with squeezing and the generation of entangled photon pairs as a source for quantum illumination. The availability of this project's JTWPAs, together with associated new and fundamental developments in Josephson quantum metamaterials (due to the further exploitation of a non-centrosymmetric nonlinearity), would enable these experiments to be realised by the scientific community after this project's lifetime.

The project has received several invitations to present its results at various prestigious events including the international workshop on 'Use-cases from quantum technologies for sensing and metrology', held in December 2018 in France and at various research centres such as the Karlsruhe Institute of Technology (KIT), in Germany (July 2019) and the Center for Axions and Precision Physics Research, Institute for Basic Science in Korea (October 2019).

Other research groups picked up the idea of a three-wave mixing JTWPA developed within this project, e.g., VTT Technical Research Centre of Finland and Aalto University published work on applications of three-wave mixing and Kerr-free Josephson metamaterials and a group from the Lomonosov Moscow State University presented a niobium based JTWPA on the EUCAS 2021 conference.

Several follow-up projects in cooperation with stakeholders of the scientific communities were acquired, among others the project DARTWARS (Detector Array Readout with Traveling Wave AmplifieRS) and AHEAD2020, aiming to develop multiplexed SQUID arrays for radio astronomy with potential application of the JTWPA as a low noise wide band amplifier.

Impact on relevant standards

Due to the early stage of electronic quantum technologies mainly realised in scientific laboratory environments, there are still no standards for superconducting quantum devices or for single microwave photons. This project has helped to generate the necessary skills and experience within the participating NMIs and spread knowledge into a wider metrological community to create the basis for future standardisation activities.

Information on progress and on the results of this project was regularly disseminated to relevant standardisation committees such as BIPM Consultative Committee for Electricity and Magnetism (CCEM), the EURAMET TC-EM (Electricity and Magnetism), including the Working Group on Strategic Planning and the sub-committee 'DC and Quantum Metrology (DC&QM)' by presentations and through several progress reports.

Two good-practice guides covering the application of the JTWPA as a versatile two-port amplifier for quantum technologies have been prepared and submitted to CCEM and TC-EM. They are available on the ParaWave website.

Longer-term economic, social and environmental impacts

Superconducting quantum devices are accepted world-wide to be a leading contender in the development of future quantum technologies, including sensing, metrology, and computing. Quantum computing can also be used to solve complex problems in a wide range of areas of impact, such as the discovery of new medicines, optimising complex networks (e.g., global supply chains), and artificial intelligence. However, the transition of quantum technologies into commercial products requires a new generation of quantum engineers who are conversant in multi-disciplinary approaches. Specific research into JTWPAs and their applications within this project supported this by developing knowledge and research expertise within Europe, together with trained scientists and engineers.

A longer-term outcome of the project will be the building of a dedicated low-temperature setup for the characterisation of parametric amplifiers and related circuitry within PTB's new Quantum Technology Competence Center (QTZ, due for completion in 2023). The QTZ will focus on the development of user-friendly and robust components for quantum sensing and metrology and on providing calibrations, services, and facilities accessible for end users. Furthermore, QTZ will offer hands-on training and seminars for quantum technology.

The new Advanced Quantum Metrology Laboratory (AQML) at NPL in Teddington is nearing completion with occupation due in 2023. Its overall aim is to expand NPL's ground-breaking research in quantum technologies. Quantum metrology at NPL will play a crucial role in bridging the gap between quantum science and industry to help grow a profitable and sustainable quantum industry deeply rooted in the UK. The AQML forms part of Quantum Metrology Institute which brings together all of NPL's leading-edge quantum science and metrology research and provides the expertise and facilities needed for academia and industry to test, validate, and ultimately commercialise new quantum research and technologies. The ParaWave Metrology Platform will be located in the AQML with close proximity to related research in quantum technologies and will form part of NPL's showcase for quantum technologies with industry in the UK and further afield.

In addition, INRIM has developed the Piemonte Quantum Enabling Technology (PiQuET, completed 2020, www.piquetlab.it) and transferred this project's fabrication processes into PiQuET. PiQuET provides 400 m^2 of clean room space for the development of new quantum, micro and nano devices, and will bring together and expand the knowledge of European scientists, engineers, and industry in Quantum Enabling Technologies.

6 List of publications

[1] S. V. Lotkhov, R. Dolata, M. Khabipov, "*DC measurement of dressed states in a coupled 100 GHz resonator system using a single quasiparticle transistor as a sensitive microwave detector*", Appl. Phys. Lett. 115, 192601 (2019) https://doi.org/10.1063/1.5119220

[2] A. B. Zorin, "*Flux-Driven Josephson Traveling-Wave Parametric Amplifier*", Phys. Rev. Applied 12, 044051 (2019) https://doi.org/10.1103/PhysRevApplied.12.044051

[3] L. Fasolo, A. Greco, and E. Enrico, "*Superconducting Josephson-Based Metamaterials for Quantum-Limited Parametric Amplification: A Review*", Condensed Matter Physics, Edited by InTech Open (2019) https://doi.org/10.5772/intechopen.89305

[4] T. Dixon, J.W. Dunstan, G.B. Long, J.M. Williams, P.J. Meeson, and C.D. Shelly, "*Capturing Complex Behavior in Josephson Traveling-Wave Parametric Amplifiers*", Phys. Rev. Applied 14, 034058 (2020) https://doi.org/10.1103/PhysRevApplied.14.034058

[5] I. Golokolenov, A. Guthrie, S. Kafanov, Yu. A. Pashkin and V. Tsepelin, "*On the origin of the controversial electrostatic field effect in superconductors*", Nat Commun 12, 2747 (2021) https://doi.org/10.1038/s41467-021-22998-0

[6] A. Greco, L. Fasolo, A. Meda, L. Callegaro and E. Enrico, "*Quantum model for rf-SQUID-based metamaterials enabling three-wave mixing and four-wave mixing traveling-wave parametric amplification*", Phys. Rev. B 104, 184517 (2021) https://doi.org/10.1103/PhysRevB.104.184517, click here for open access full text

[7] A. B. Zorin, "*Quasi-phasematching in a poled Josephson traveling-wave parametric amplifier with three-wave mixing*", Appl. Phys. Lett. 118, 222601 (2021) https://doi.org/10.1063/5.0050787, click here for open access full text

[8] L. Fasolo, A. Greco, E. Enrico, F. Illuminati, R. Lo Franco, D. Vitali, P. Livreri, "*Josephson Traveling Wave Parametric Amplifiers as Non-Classical Light Source for Microwave Quantum Illumination*", Measurement: Sensors 18, 100349 (2021) https://doi.org/10.1016/j.measen.2021.100349

[9] L. Fasolo, C. Barone, M. Borghesi, G. Carapella, A. P. Caricato, I. Carusotto, W. Chung, A. Cian, D. Di Gioacchino, E. Enrico, P. Falferi, M. Faverzani, E. Ferri, G. Filatrella, C. Gatti, A. Giachero, D. Giubertoni, A. Greco, C. Kutlu, A. Leo, C. Ligi, P. Livreri, G. Maccarrone, B. Margesin, G. Maruccio, A. Matlashov, C. Mauro, R. Mezzena, A. G. Monteduro, A. Nucciotti, L. Oberto, S. Pagano, V. Pierro, L. Piersanti, M. Rajteri, A. Rettaroli, S. Rizzato, Y. K. Semertzidis, U. Uchaikin, A. Vinante, "*Bimodal Approach for Noise Figures of Merit Evaluation in Quantum-Limited Josephson Traveling Wave Parametric Amplifiers*", IEEE Transactions on Applied Superconductivity 32 (4) 1700306 (2022) https://doi.org/10.1109/TASC.2022.3148692

[10] M. Khabipov, V. Gaydamachenko, C. Kissling, R. Dolata and A. B. Zorin, "*Superconducting microwave resonators with non-centrosymmetric nonlinearity*", Superconductor Science and Technology 35, 065020 (2022) https://doi.org/10.1088/1361-6668/ac6989

[11] S. Wolter, J. Linek, T. Weimann, R. Kleiner, D. Koelle, R. Kleiner and O. Kieler, "*Static and dynamic transport properties of multi-terminal, multi-junction microSQUIDs realized with Nb/HfTi/Nb Josephson junctions*", Superconductor Science and Technology (2022) https://doi.org/10.1088/1361-6668/ac782b

[12] AP. Livreri, E. Enrico, L. Fasolo, A. Greco, A. Rettaroli, D. Vitali, A. Farina, F. Marchetti, D. Giacomin, "*Microwave Quantum Radar using a Josephson Traveling Wave Parametric Amplifier*", 2022 IEEE Radar Conference RadarConf22 (2022) https://doi.org/10.1109/RadarConf2248738.2022.9764353, click here for open access full text

This list is also available here: https://www.euramet.org/repository/research-publications-repository-link/

7 Contact details

After July 2022 the coordinator will no longer be available.

Please contact Marat Khabipov (Marat.Khabipov@ptb.de) or Mark Bieler (Mark.Bieler@ptb.de).